BRAIN CONNECTIVITY
Volume 6, Number 6, 2016

DOI: 10.1089/brain.2015.0375

Implication of the Slow-5 Oscillations in the Disruption of the Default-Mode Network in Healthy Aging and Stroke

Christian La,[1,2] Veena A. Nair,[2] Pouria Mossahebi,[2] Brittany M. Young,[1,2] Marcus Chacon,[3] Matthew Jensen,[3] Rasmus M. Birn,[1,4,5] Mary E. Meyerand,[1,2,4,6] and Vivek Prabhakaran[1–6]

Abstract

The processes of normal aging and aging-related pathologies subject the brain to an active re-organization of its brain networks. Among these, the default-mode network (DMN) is consistently implicated with a demonstrated reduction in functional connectivity within the network. However, no clear stipulation on the underlying mechanisms of the de-synchronization has yet been provided. In this study, we examined the spectral distribution of the intrinsic low-frequency oscillations (LFOs) of the DMN sub-networks in populations of young normals, older subjects, and acute and subacute ischemic stroke patients. The DMN sub-networks were derived using a mid-order group independent component analysis with 117 eyes-closed resting-state functional magnetic resonance imaging (rs-fMRI) sessions from volunteers in those population groups, isolating three robust components of the DMN among other resting-state networks. The posterior component of the DMN presented noticeable differences. Measures of amplitude of low-frequency fluctuation (ALFF) and fractional ALFF (fALFF) of the network component demonstrated a decrease in resting-state cortical oscillation power in the elderly (normal and patient), specifically in the slow-5 (0.01–0.027 Hz) range of oscillations. Furthermore, the contribution of the slow-5 oscillations during the resting state was diminished for a greater influence of the slow-4 (0.027–0.073 Hz) oscillations in the subacute stroke group, not only suggesting a vulnerability of the slow-5 oscillations to disruption but also indicating a change in the distribution of the oscillations within the resting-state frequencies. The reduction of network slow-5 fALFF in the posterior DMN component was found to present a potential association with behavioral measures, suggesting a brain–behavior relationship to those oscillations, with this change in behavior potentially resulting from an altered network integrity induced by a weakening of the slow-5 oscillations during the resting state. The repeated identification of those frequencies in the disruption of DMN stresses a critical role of the slow-5 oscillations in network disruption, and it accentuates the importance of managing those oscillations in the health of the DMN.

Key words: aging; default-mode network; fALFF; posterior DMN; rs-fMRI; slow-5; stroke

Introduction

Contemporary functional neuroimaging techniques, such as functional magnetic resonance imaging (fMRI), provide excellent opportunities for the noninvasive investigation of the human brain. Of these, the development of resting-state fMRI (rs-fMRI) has proved particularly advantageous for the study of impaired populations, as no active task participation is required. In this study, we defined *resting state* as a condition in which participants are not instructed to attend to any specific task, hence requiring minimal subject compliance. The approach of rs-fMRI reduces the influence of known task-related confounds such as subjects' variability in a number of factors (effort, attention, motivation, performance, etc.), and it allows for an investigation of the intrinsic functional networks that is both consistent and reliable (Damoiseaux et al., 2006; Patriat et al., 2013; Van Dijk et al., 2010).

Functional connectivity (Friston et al., 1993), an approach implemented in the analysis of rs-fMRI, measures the correlation, or level of synchronization, between signals from distal brain regions (Biswal et al., 1995), with high synchronization suggesting shared function. Functional connectivity allows for the depiction and identification of spatially

[1]Neuroscience Training Program, University of Wisconsin-Madison, Madison, Wisconsin.
Departments of [2]Radiology, [3]Neurology, [4]Medical Physics, [5]Psychiatry, and [6]Biomedical Engineering, University of Wisconsin-Madison, Madison, Wisconsin.

distinct but functionally related regions, forming diverse, robust, and intrinsic functional networks of the cortical system, which are also known as the resting-state networks (RSNs) (Beckmann et al., 2005; Birn et al., 2013; Damoiseaux et al., 2006; Fox and Raichle, 2007).

One of the more investigated RSNs, the default-mode network (DMN) is generally considered as a collection of subsystems usually suppressed in goal-directed behavior (Fox and Raichle, 2007; Raichle et al., 2001), but it also has a role in mind-wandering (Raichle et al., 2001), episodic memory (Buckner et al., 2008; Wagner et al., 2005), introspection, and self-referential processes (Andrews-Hanna et al., 2010; Buckner et al., 2008; Fransson, 2005; Gusnard et al., 2001a; Johnson et al., 2005; Qin and Northoff, 2011; Schmitz et al., 2004). Comprising the precuneus/posterior cingulate cortex (pC/PCC) complex, the medial prefrontal cortex (mPFC), and bilateral inferior parietal lobules (IPLs) as its core regions, the DMN is also the intrinsic network that is the most activated during the state of *rest*, making it a prime target for investigation in healthy and clinical populations.

Perturbation of this DMN in resting conditions (Damoiseaux et al., 2008; Ferreira and Busatto, 2013; Koch et al., 2010), as well as under task conditions (Grady et al., 2006; Persson et al., 2007), has been consistently associated with the process of normal aging as well as with age-related brain changes. Changes in the DMN have furthermore been linked with insidious pathological changes in clinical populations of progressive neurological disorders (e.g., Alzheimer's disease, Autism spectrum disorders, Parkinson's disease, Schizophrenia, etc.) (Broyd et al., 2009; Greicius, 2008).

Of the reported abnormalities, this network has been shown to exhibit decreases in cortical activation during a state of resting, whereas a reduction in deactivation is found during performance of a task, marking a possible failure of the system to disengage task-irrelevant systems and contributing to a potential increase in cortical system noise and a decrease in overall DMN functionality in the elderly and disease populations (Grady et al., 2006; Meinzer et al., 2012; Persson et al., 2007). This deficit in activation/deactivation pattern has also been shown to be coupled with a reduction in the synchronicity of the intrinsic oscillations in regions comprising the network (He et al., 2007; Sambataro et al., 2010), reflecting a reduction in DMN functional integrity. Such changes are particularly evident in the pC/PCC complex, not only a proven core region functionally (Andrews-Hanna et al., 2010; Raichle et al., 2001) but a core region metabolically as well (Gusnard et al., 2001b; Raichle, 2010).

Recently, several investigations have described similar disruptions of the DMN in stroke populations, in terms of reduced network co-activation, regional homogeneity, and amplitude of low-frequency fluctuations (ALFF) (Park et al., 2014; Tsai et al., 2014; Tuladhar et al., 2013; Wang et al., 2014). In contrast to the process in normal aging and in other previously recorded populations exhibiting DMN disruption, ischemic stroke is a nonprogressive vascular injury imposing an acute and rapid reorganization of the cortical system, thus contributing to the interest of this investigation. Despite presenting similar signs of DMN disruption, the mechanism underlying the network disruption remains unclear, and whether the mechanism after the onset of a stroke is comparable to that in normal aging is currently unknown.

In this study, we provided an investigation of the DMN disruption in these two populations (aging and stroke) in terms of characteristics of the frequency distribution of the intrinsic low-frequency oscillations (LFOs). Deviating from pure assessment of synchronicity, our investigation involved four population categories (two healthy normal populations differentiated by age, and two stroke populations differentiated by their time from stroke onset), with the aim of uncovering the power spectrum characteristics underlying the disruption of the network.

Currently, the methods of ALFF (Yang et al., 2007) and fractional ALFF (fALFF) (Zou et al., 2008) have been used to describe spectral characteristics. These methods implement voxel-wise approaches to estimate the spectral power and relative spectral power, respectively, of oscillations within frequencies of a certain range (commonly in the 0.01–0.08 Hz range for the resting-state frequencies), and they provide summative measures. Analysis of the frequency distribution (or spectral analysis) of the LFOs could provide additional information regarding characteristics of the intrinsic cortical fluctuations such as distribution peak, distribution width, and distribution skewness among other measures to aid the characterization of the disruption.

Moreover, implementation of such analyses on oscillations of independent component analysis (ICA)-derived components provides additional reliability and consistency for a comparison between the groups. This method also allows for the investigation of network-specific oscillations, comparable to an ROI-based approach with functionally defined regions. Under such an approach, the investigation provides an analysis on the representative oscillations from hundreds of voxels comprising the network. From this approach, we hypothesized that disruption of the frequency distribution within the DMN will be noted in our aging and stroke groups, with such a disruption arising from a change in either the amplitude or the frequency of the distribution peak, ultimately interfering with network synchronization between remote regions.

Materials and Methods

Participants

One hundred and thirty-seven participants were included in this cross-sectional study. Each participant was asked to participate in an MRI session, including a resting-state fMRI scan with eyes-closed conditions and a high-resolution structural MRI scan (see MRI acquisition section for scan parameters). Resting fMRI sessions with excessive motion (exceeding 2 mm in any of the x-y-z and angular directions) and/or presenting gross artifacts (ghosting, shimming, susceptibility, calcification artifacts, etc.) were excluded. As a result, sessions from 18 of those participants were excluded from analysis. Two of the stroke subjects presented lesions pertaining to regions in the vicinity of primary oscillator regions of the DMN (PCC and mPFC), potentially influencing the DMN components' oscillations, and were, therefore, removed from the study analysis.

The remaining 117 individual sessions made up four population categories: (1) young healthy adult subjects ($n = 43$), (2) older healthy adult subjects ($n = 42$), (3) adults with acute stroke (≤7 days from stroke onset, $n = 14$), and (4) adults with sub-acute stroke (between 10 days and 7 months from stroke onset, $n = 18$). Participants' details can be found in Table 1.

Table 1. Subjects' Demographic Table

	Sample size, n	*Gender*	*Mean age (years)*	*Time after stroke onset*	*NIH-SS*
Young normals	43	23 M: 20 F	22.5 ± 2.7	n/a	n/a
Old normals	42	22 M: 20 F	61.2 ± 7.8	n/a	n/a
Acute stroke patients	14	11 M: 3 F	65.0 ± 15.7	4.6 ± 1.91 days	3.4 ± 5.0
Subacute stroke patients	18	10 M: 8 F	58.9 ± 11.2	14 ± 8.8 weeks	2.6 ± 3.8

Gender differences not significant (chi-square test, $p = 0.61$).
n/a, not applicable; NIH-SS, National Institute of Health Stroke Scale.

Details regarding clinical, demographic, and session information for the 34 enrolled ischemic stroke patients can be found in Supplementary Table S1 (Supplementary Data are available online at www.liebertpub.com/brain). No stroke subject was repeatedly scanned between the acute and subacute time-points in this analysis. A lesion density map, derived from semi-automated segmentation from available T1 BRAVO, Cube T2 FLAIR, and Diffusion-Weighted Image (DWI) using Jim 7 (Xinapse, www.xinapse.com), was created and describes the lesion location and lesion overlap between the 32 stroke subjects (Fig. 1). No considerable overlap was present among lesions from the 32 stroke patients, with maximum overlap of two lesions recorded at any given spatial location (Fig. 1, cyan).

The difference in age between the young group and each of the other groups (older healthy individuals, acute and subacute patients) was significant (*t*-test, $p < 0.001$), which allowed for the assessment of an age effect. No significant difference in age was found between the old, acute, and subacute stroke groups, therefore controlling for age as a factor in our investigation of stroke-related brain changes. From an estimate using the Euclidean norm, head motion was found to differ between the age groups, with older participants (older healthy adults and stroke patients) exhibiting larger motion (Supplementary Fig. S1). A difference in head motion between our healthy older adults and our adults with stroke (acute and subacute) was of no significance, minimizing the concern of head motion dramatically influencing our spectral characteristic measures.

The inclusion of a young healthy group permitted a distinction between an age effect (assessable with a healthy young versus healthy older adults comparison) and a stroke effect (assessable with a healthy old versus stroke groups comparison). Two separate sets of stroke patients (acute and subacute) were included, permitting an investigation of the changes over the DMN—a network central to the cortical system—over different stages after stroke onset. Because of its deeper core structure and high vascularization, the DMN exhibits lower stroke susceptibility than other regions, which is advantageous in an investigation of remote (diaschisis) effects of stroke from regions outside of the DMN.

No significant difference in the National Institute of Health Stroke Scale (NIH-SS) scores was noted between the acute and subacute stroke groups, with patients predominantly having only mild impairments (Table 1). Recruited participants in this study expressed no history or signs of psychological or psychiatric disorders with no participant presenting signs of compromised capacity or ability to consent, as established by neurological examination. All participants provided written informed consent toward participation in compliance with the University of Wisconsin-Madison Health Sciences Institutional Review Board (IRB).

MRI acquisition

All neuroimaging data were collected at the University of Wisconsin-Madison, using two identical 3.0-Tesla GE Discovery MR750 scanners (GE Healthcare, Waukesha, WI) equipped with an 8-channel head coil. Each participant underwent an MRI scanning session, which included a 10-min eyes-closed resting-state scan and a high-resolution 3D structural scan. The 3D high-resolution axial structural scan was acquired using a T1-weighted IR-prepared SPGR BRAVO sequence with 156 slices, isotropic $1 \times 1 \times 1\ mm^3$ with slice thickness = 1 mm, over a 256×256 matrix, TR = 8.132 ms, TE = 3.18 ms, TI = 450 ms, FOV = 256 mm, and

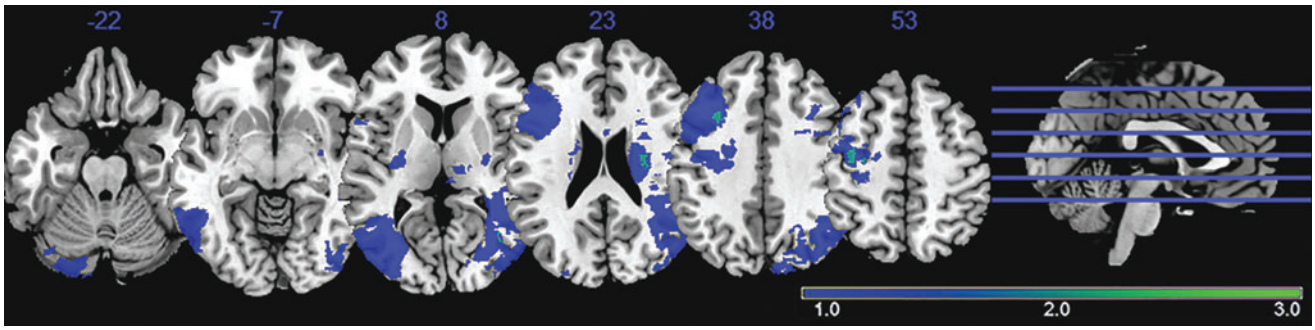

FIG. 1. Lesion density map for 32 ischemic stroke patients (acute and subacute combined), with dark blue representing a single lesion, and light blue representing overlap of two lesions. No regions demonstrated more than two lesions overlapping. Two subjects exhibited lesions in regions of the DMN and were, therefore, removed from the analysis. Neurological convention: Left is left. DMN, default-mode network.

flip angle = 12°. The 10-min resting fMRI scans were obtained using single-shot echo-planar T2*-weighted gradient-echo echo planar imaging, with 40 sagittal slices, TR = 2.6 s, TE = 22 ms, FOV = 224 mm, flip angle = 60°, and isotropic 3.5 mm^3 voxel. Earplugs and foam padding were used to attenuate scanner noise and to minimize head movement, respectively. Subjects were also reminded to hold their head still and minimize head motion before the start of every scan.

Data preprocessing

The MR data preprocessing was achieved using Data Processing Assistant for Resting-State fMRI (DPARSFA v2.3; [19]) and SPM8 (Wellcome Trust Centre for Neuroimaging, University of College London, United Kingdom). The first 10 volumes were discarded. The remaining images were slice-time corrected and spatially realigned. Data spikes were removed using AFNI's 3dDespike (http://afni.nimh.nih.gov/afni/). The image volumes were normalized to an MNI EPI template using linear, then nonlinear registration, and smoothed with a 4-mm Gaussian kernel using SPM8 software. CSF and white matter signals, and other known nuisance covariates (e.g., motion), were not regressed out of the signal before group independent component analysis (groupICA), as regression of those known nuisance covariates would significantly reduce ICA's ability to isolate the various noise components and to remove the contribution of those noise components from the signal of interest. Head motion in the participants was also computed using the Euclidean norm (enorm—square root of the sum squares) approach to assess the possible contribution head motion in our results from the spectral analysis.

Group independent component analysis

groupICA was implemented with GIFT(v2.0a) Matlab software (http://mialab.mrn.org/software/gift/). The approach was modeled with an unconstrained mid-order 28 independent component model using the *Infomax* algorithm, default mask file, standard PCA type, and back-reconstruction using groupICA method. The *Infomax* algorithm incorporates nonlinearities in the transfer function to capture higher-order moments (Bell et al., 1995), and it is used to detect the independent source components of the rs-fMRI data. Reliability of the ICA algorithm was assessed with the ICASSO toolbox (www.cis.hut.fi/projects/ica/icasso) (Himberg et al., 2004), with 20 iterations of the ICA using *RandInit* and *Bootstrap* methods. Group ICA generated a representative time-series for each of the independent components isolated from the dataset and its corresponding spatial map that is then back-projected onto individual spatial maps. From the 28 independent component model, multiple components of the DMN were identified and isolated, similar to those presented in Allen et al. (2011), and they were kept segregated from one another to differentiate among sub-networks. This study focused primarily on the posterior DMN (pDMN) subsystem, our most robust component of the DMN.

Spectral analysis

Computing measures of LFOs in the frequency domain has the advantage of offering the ability to simultaneously examine specific bands within the resting-state frequencies (0.01–0.08 Hz). Similar to a method described in Allen et al. (2011), back-reconstructed IC time-series from each individual were converted by Fast Fourier Transform to obtain their component spectra. Furthermore, a Gaussian filter with $\sigma = 2$ was applied to smooth the power spectra histogram to reduce the influence of unnatural spikes in the distribution.

To examine the difference in power spectra between the populations, six descriptive univariate measurements were assessed: (1) frequency of the spectral peak as the component peak oscillation frequency, (2) FWHMx as the width of the distribution of the oscillations in the frequency axis, (3) skewness as the shape of the distribution of the LFO intensity, (4) peak amplitude as the power of the peak oscillation, (5) component ALFF as an index of LFO intensity within the resting-state frequency range, incorporating slow-5 and slow-4 (total frequency range: 0.01–0.073 Hz), and (6) component fALFF as a normalized measure of the relative contribution of those oscillations to the whole detectable range, computed by dividing cortical oscillation amplitude by the total cortical power recorded over the spectrum.

This latter method has been suggested to reduce the contribution from physiological noise that is irrelevant to brain activity on the signal of interest, in particular in the region of the PCC with its close proximity of large draining blood vessels, therefore providing an improved sensitivity and specificity in detecting spontaneous brain activities (Zou et al., 2008). In this study, the measures of ALFF (Yu-Feng et al., 2007) and fALFF (Zou et al., 2008) are amplitude measured from representative component time-series and not voxel-wise time-series.

The resting-state frequencies were further divided into the slow-5 (0.01–0.027 Hz) and slow-4 (0.027–0.073 Hz) bands after the discovery of the natural logarithmic relationship between brain oscillators by Buzsaki and colleagues (Buzsáki and Draguhn 2004; Penttonen and Buzsáki, 2003). In this study, we provided an application of ALFF and fALFF metrics not on fluctuations from a single voxel but on the representative oscillation signature of the group ICA-derived component, drawing information from the many voxels comprising the sub-network, allowing for a stable representation of the network oscillation characteristics. We considered resting-state frequencies as a strict combination of slow-5 and slow-4 frequencies (0.01–0.073 Hz), unless specified. The relative contribution of slow-5 was computed by (slow-5 fALFF)/[(slow-5 fALFF) + (slow-4 fALFF)].

Statistical analyses

For each descriptive measure to be assessed, single-factor analysis of variances (ANOVAs) were conducted with the group serving as the single factor (young, old, acute stroke, subacute stroke). A single-factor ANOVA was chosen because of the nonindependence of the six measures, since each of the measures pertains to a single frequency distribution. A *post hoc* Tukey's honest significant difference (HSD) test was implemented to assess the significance of the difference of the means between population groups. Discrete frequency bin analyses were also utilized in the investigation of group mean spectra, where amplitudes at each of the frequency bins from 0.009 to 0.0450 Hz, with a bin size of $\sim$0.0015 Hz, and were tested using Student's two-sample *t*-tests (12 bins in the slow-5 and 12 bins in the slow-4).

Table 2. Identification of Default-Mode Network Sub-Networks

Name	*DMN Corr.*	*($Power_{LF}$)/ ($Power_{HF}$)*
Posterior DMN	0.529	80.510
Ventral DMN	0.309	53.419
Anterior DMN	0.259	60.13
Ventral-anterior DMN*	0.319	20.113
1° visual network	0.068	183.183
Sensorimotor network	0.037	87.042

Independent component analysis-derived networks resembling the DMN with respective correlation and regression values to the provided DMN mask template (dmn_mask_calhoun.nii) in GIFT. Values for DMN components show moderate correlations to the template; primary visual cortex and sensorimotor network demonstrate low DMN correlations, and they are provided here for comparison. Ventral-anterior DMN labeled with the "*" presented low robustness and will not be discussed in this study.

DMN, default-mode network.

Results

Functional networks

Group ICA with a mid-order 28 independent component model allowed for the identification of 21 non-noise, functionally relevant, and spatially and temporally segregated components in accordance with network templates from a previous study (Allen et al., 2011). These 21 components accounted for 89.1% of the total observed variance in the data, and they consisted, in part, of the DMN, sensorimotor, auditory, visual (lower- and higher-order components), and attention networks. The relevance of the DMN to aging and various disease populations provided motivation to concentrate our effort in the study on the DMN and its sub-systems.

Of the 28 independent components, four components provided resemblance to that of the DMN with their correlation value to the DMN template provided in Table 2. One of those four components presented weak robustness of the component with a markedly lower (power of the low-frequency [resting-state frequencies: 0.01–0.1 Hz]/power of the high-frequency [0.1–0.192 Hz]) ratio compared with the others (Tables 1 and 2), and it will not be discussed further. Despite sharing comparable spatial distribution encompassing the pC/PCC, the medial PFC, and the bilateral IPLs, these DMN components offered distinct spatiotemporal features (Fig. 2). We identified these three components as the precuneus/pDMN, the medial PFC/anterior DMN (aDMN), and the retro-splenial/ventral DMN (vDMN), listed in Table 2, with their correlation to a DMN template in GIFT (dmn_mask_calhoun.nii) (Allen et al., 2011). The next highest correlations to the DMN template pertained to components of the salience and visual network, and these were of much lower correlational values.

Spectral analysis: characteristics of the spectral distribution

Spectral analysis of the LFOs offers an alternative approach for the understanding of functional network dynamics. Despite high levels of noise persisting in the spectral analysis of the LFOs, in particular in acute and subacute stroke populations of a low sample size, group mean spectra displayed stable oscillation distribution patterns within each group, allowing characterization of the disparity among the groups. A graphical representation of the pDMN power spectrum (Fig. 3) depicted three observations: (1) a possible age-related shift in peak oscillation frequency, (2) a stroke-related depression of fluctuation amplitude apparent in the subacute stroke population, possibly accompanied by (3) a broadening of the spectral distribution. The components of aDMN, vDMN, visual network, and motor network components demonstrated a similar pattern of reduced oscillation amplitudes, but with no demonstration of a shift in frequency of the peak and no evidence of a broadening of the distribution (Fig. 4). For the purpose of this study, we

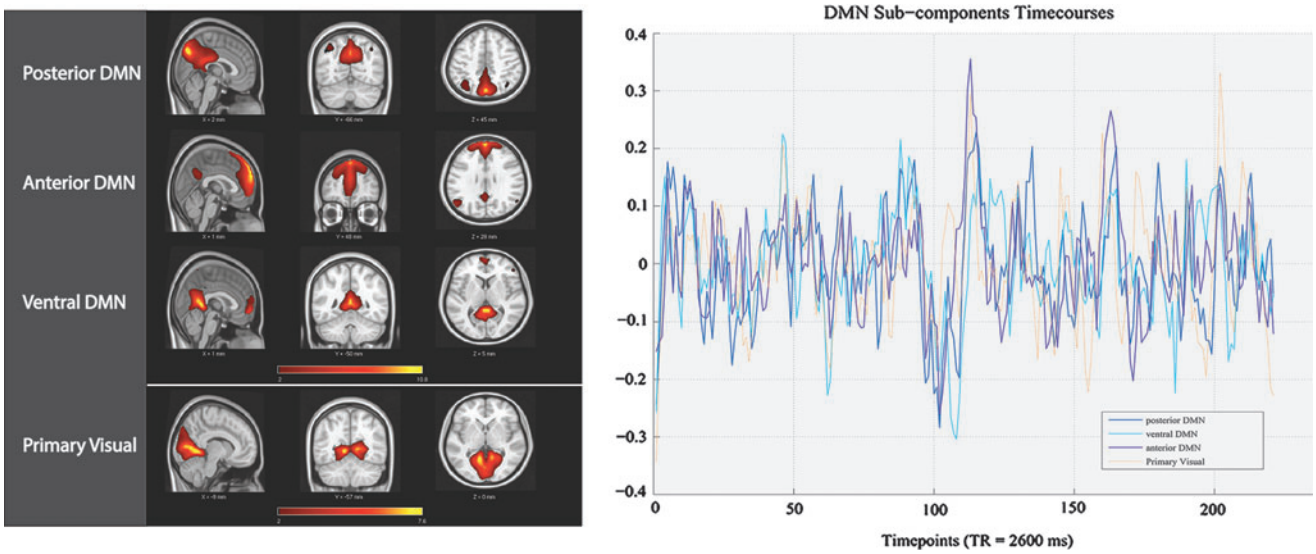

FIG. 2. Comparative spatial maps and time-series for three DMN sub-networks and the primary visual network. Left: DMN and primary visual sub-components' spatial maps. Right: DMN and primary visual sub-components' time-series. Despite sharing similarities, the three subcomponents of the DMN exhibit small but distinct spatiotemporal differences. Spatial map and time-series for the visual components shown here are for comparative purposes.

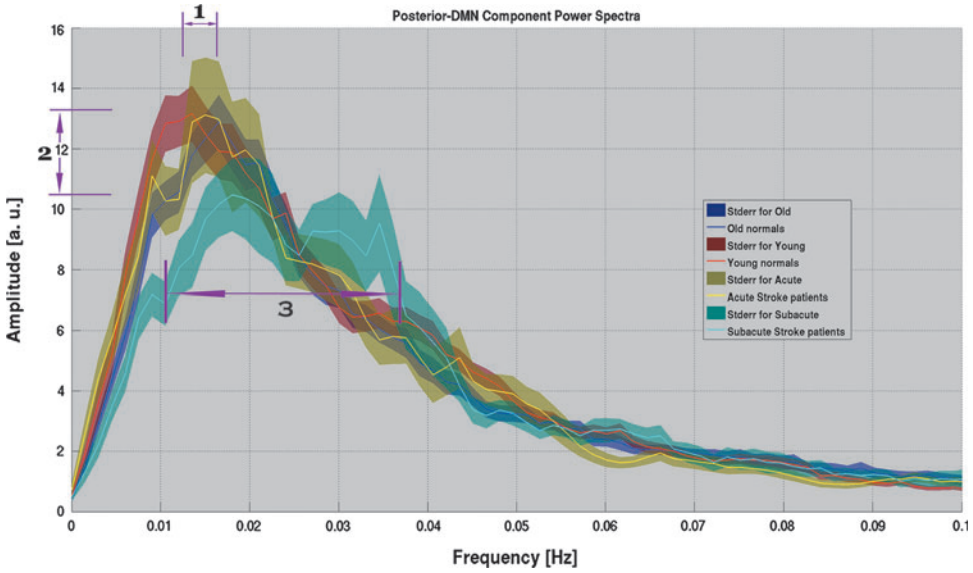

FIG. 3. Power spectra of the posterior DMN (pDMN) component for each of the population groups. Shaded area represented standard error of the means. This plot illustrates: (1) a possible shift in distribution peak in the aging population, and (2) a reduction in amplitude of the spectral peak coupled with (3) a broadening of the spectral peak distribution in the sub-acute stroke patients.

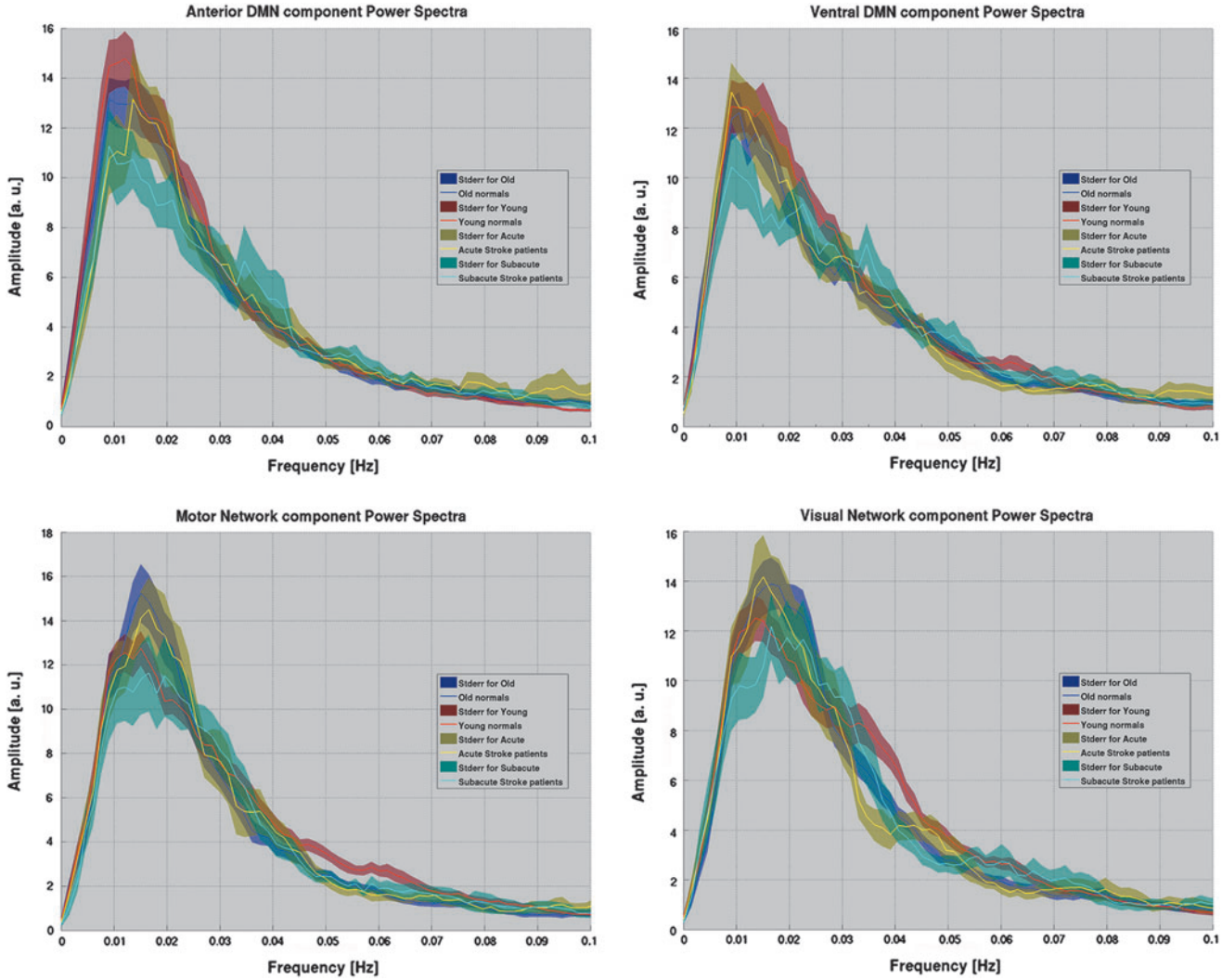

FIG. 4. Power spectra for other network components showing a reduction in amplitude, but no shift in frequency, of the spectral peak. Top: The anterior DMN (left) and ventral DMN (right). Bottom: Sensorimotor (left) and visual (right) networks for comparison, with each population similarly color coded. In contrast, pDMN observed a reduction in amplitude and a shift in frequency as noted in Figure 2.

focused the current investigation on the posterior component of the DMN, our most robust sub-component of the DMN.

Individual subjects' spectral distribution was assessed using the six descriptive univariate measurements previously described (see spectral analysis). A single-factor ANOVA revealed lack of statistical significance between the groups in the measures of frequency of the peak ($F = 1.598$, $p = 0.194$), distribution width ($F = 0.031$, $p = 0.993$), distribution skewness ($F = 0.642$, $p = 0.590$), amplitude of the peak ($F = 1.449$, $p = 0.232$), and the estimate of resting-state oscillation power with ALFF ($F = 1.568$, $p = 0.201$). Though not of statistical significance, spectral distribution of the young population group peaked at a lower mean frequency of 0.018 Hz; whereas the old population group peaked at 0.024 Hz; acute stroke, at 0.021 Hz; and subacute stroke, at 0.027 Hz (Fig. 5A), demonstrating a tendency of higher oscillation in older participants. Differences in distribution width and distribution skewness were insignificant and negligible.

An analysis of the amplitude of the power spectra distribution appears to show a group-mean decrease in amplitude of the spectral peak in the old group compared with the young group (Fig. 5D); the effect was also not statistically significant ($F = 1.449$, $p = 0.232$). Amplitude of the mean spectra was elevated to 15.583 a.u. (arbitrary unit) for the young group and was only 13.898 a. u. for the old group. Similarly, measures of ALFF showed a similar mean decrease in the older group compared with the younger group, with the effect not reaching statistical significance ($F = 1.568$, $p = 0.201$) (ALFF means, Young = 265; Old = 250; Acute = 254; Subacute = 249) (Fig. 5E). In contrast, fALFF, an adjusted metric of power of the oscillations, showed a significant difference between the groups ($F = 3.457$, $p = 0.018$), with differences emanating primarily from older versus young healthy adults (Tukey HSD, $p = 0.043$) and from subacute patients versus young healthy adults (Tukey HSD, $p = 0.043$), demonstrating lower oscillation power in those populations (Fig. 5F, bottom right), with the subacute stroke group having not only a lower mean but also greater standard deviation.

Spectral analysis: slow-5 and slow-4 oscillations

Distinction of the resting-state slow-5 (0.01–0.027 Hz) and slow-4 (0.027–0.073 Hz) components allowed for an assessment of the power distribution within the resting-state frequencies (0.01–0.073 Hz). The estimates of slow-5 and slow-4 power, however, did not affirm differences between the groups (slow-5: $F = 1.780$, $p = 0.155$; slow-4: $F = 1.378$, $p = 0.253$) (Fig. 6). Within the frequency bands, the slow-5 frequencies exhibited a pattern of lower amplitude in their oscillations, and the slow-4 oscillations displayed an amplitude increase in the subacute stroke population. Together, they contribute to a change in the relative contribution of slow-5 and slow-4 in the resting-state fluctuations of the subacute stroke group (subacute vs. old t-test, $t_{31} = 2.146$, $p = 0.039$), disrupting the established dominance of slow-5 in healthy adults (Zuo et al., 2010).

The spectral distribution was further investigated via an analysis of discrete frequencies (Fig. 7, bottom). Figure 7 offers an illustration of mean power spectra (Fig. 7, top) and

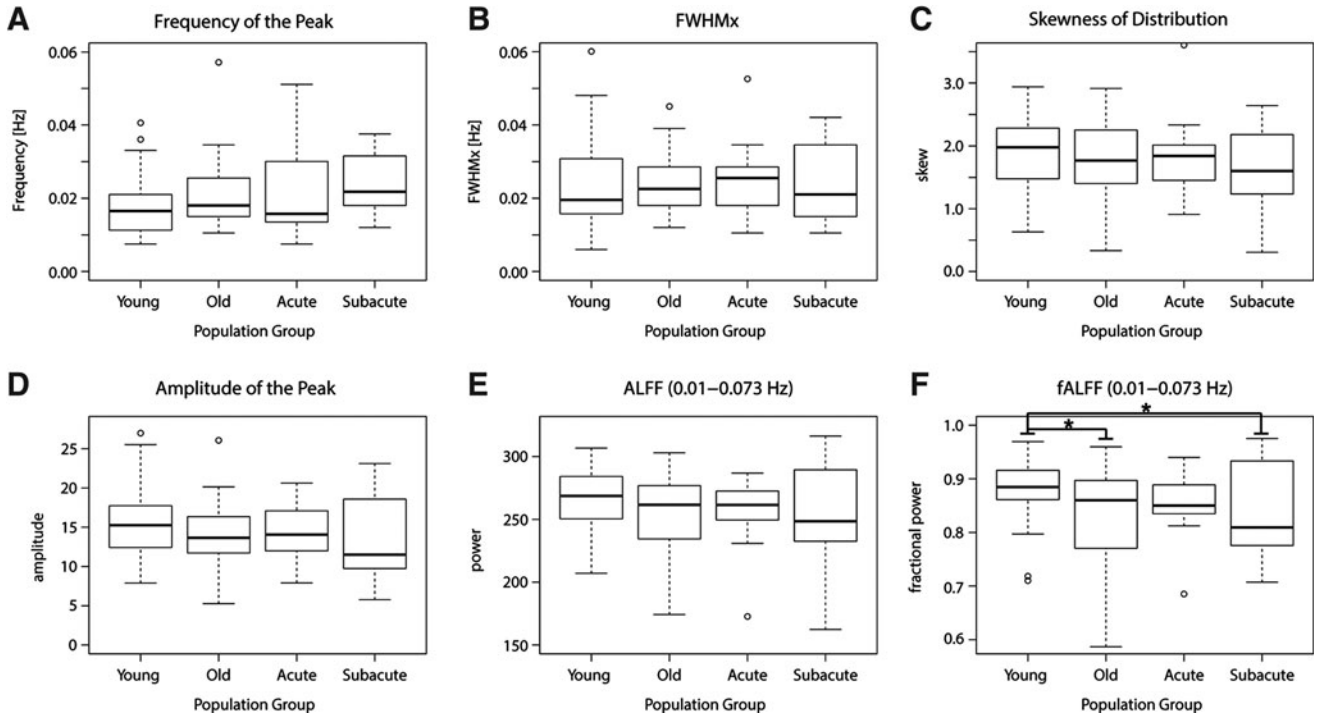

FIG. 5. Six measures descriptive of frequency distribution characteristics. Top row: **(A)** Frequency of the spectral peak, **(B)** Full-width half-max, and **(C)** Distribution skewness. Bottom row: **(D)** Amplitude of the spectral peak, **(E)** ALFF between 0.01 and 0.073 Hz, and **(F)** fractional ALFF between 0.01 and 0.073 Hz. Actually tested range was 0.009–0.0736 Hz due to discretization of the frequencies. Statistical significance: $*p < 0.05$. All six measures were derived from spectra smoothed with Gaussian filter ($\sigma = 2$). Open circles signify data-points that fell outside the whiskers. ALFF, amplitude of low-frequency fluctuation.

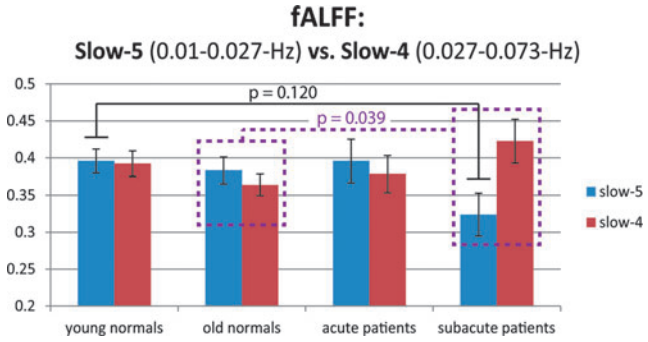

FIG. 6. Slow-5 and slow-4 fractional ALFF for pDMN in each of the population groups. Blue denotes slow-5 (0.01–0.027 Hz). Red denotes slow-4 (0.027–0.073 Hz). Pattern of a reduction in fALFF in the subacute stroke group was observed in comparison to the other population groups (Tukey honest significant difference, $p = 0.12$), whereas component slow-4 fALFF increased. Differences were also suggested in terms of the relative contribution of the slow-5 to that of the slow-4 oscillations when comparing the subacute stroke group with the older adult group (unpaired two-sample *t*-test, $t_{31} = 2.146$, $p = 0.039$, dotted line/box). In that group, the slow-4 constituent of the intrinsic oscillations was noted as becoming the dominant contributor within the resting-state frequencies. fALFF, fractional ALFF.

smoothed power spectra (Fig. 7, middle). The differences between the mean of the different populations were assessed for significance using Student's two-sample *t*-tests in steps of ~ 0.0015 Hz between the frequencies from 0.009 to 0.027 Hz and from 0.027 to 0.045 Hz, as represented by the rectangular boxes in the lower portion of Figure 7. For each of the subtractions (Old minus Young, Subacute Stroke minus Young, and Subacute Stroke minus Old), the largest difference resided in the lower frequencies of the slow-5 frequency range (Fig. 7, bottom, $p < 0.05$). Moreover, a significant residual peak in the early slow-4 frequency range (~ 0.034 Hz) for the subacute stroke patients (Subacute minus Old, $p < 0.05$) demonstrates a broader range of oscillations within the pDMN.

Brain–behavior relationship

The observed network fALFF within the slow-5 oscillation range showed correspondence with the following behavioral data. The subacute stroke patients were categorized as either mild (NIHSS <2, mild stroke, $n = 7$) or moderate to severe (NIHSS ≥2, moderate to severe, $n = 10$) in terms of stroke severity; difference between the means of the slow-5 fALFF was found to be significant between these two groups ($t_{15} = 2{,}488$, $p = 0.025$). This result may be underpowered, and normality of the distributions cannot be assumed, but it suggests a possible correspondence to behavior. Regression of out-of-scanner behavior data (phonemic verbal fluency) allowed for additional characterization of brain–behavior relationships. A trend toward significance was found for the regression for phonemic verbal fluency scores, with lower scores associated with lower-network slow-5 fALFF ($R^2 = 0.329$, $F_{15} = 7.365$, $p = 0.016$) (Fig. 8).

Discussion

In the investigations of functional intrinsic networks, the DMN and other RSNs are defined by their synchronous oscillations. In a healthy system, the correlation in oscillations between regions is reflective of the strength and integrity of the functional network. However, the integrity of the system becomes disrupted in aging and in clinical populations, as seen by reduced functional connectivity between network seeds and decreased network co-activation (Andrews-Hanna et al., 2007; Broyd et al., 2009; Damoiseaux et al., 2008; Greicius et al., 2004; Greicius, 2008). Other deficits are also present, such as deficit in regional coherence (Bai et al., 2008; Zhang et al., 2012) and in intrinsic cortical activity (Han et al., 2011; Hu et al., 2014; Wang et al., 2011). However, there have been few investigations of LFOs and their amplitude information. There have been even fewer reported investigations of the frequency distribution of those oscillations. In this study, we reviewed the disruption of the DMN, and more specifically the posterior component of the DMN (pDMN), with the hypothesis that spectral characteristics of this network are being disrupted with the progression of normal aging and after the event of an ischemic stroke.

An analysis of the power spectra revealed a consistent distribution in which oscillations below 0.03 Hz contributed to the bulk of the fluctuations in the resting brain. However, the distribution of those oscillations is subject to variation, and it differs among the separate population groups (Figs. 3 and 4). Initial observations of the pDMN power spectra (Fig. 3) led us to evaluate: (1) whether frequency of the peak may be shifted with increasing age, (2) and whether amplitude is reduced and potentially coupled with (3) a broadened spectra after a stroke, prompting our investigation of distinct descriptive measures of the distribution. Many of the assessed measures for power spectra characteristics, such as distribution peak frequency, width, and skewness, did not demonstrate disparity between the populations. Evaluation of the distribution peak amplitude suggested a possible decrease in oscillation amplitude in the subacute stroke group. However, the effect did not reach significance. Less susceptible to variability, the measure of ALFF is computed through the square root of the amplitude squared within the resting-state frequency range. However, this measure may be heavily confounded by physiological noise. This concern is particularly valid while investigating the pDMN with the PCC as the main oscillator, due to close proximity to large draining vessels.

fALFF provided an improvement on the measure by taking the ratio of the power within the frequencies of interest to that of the whole assessed frequency range, delivering a measure with improved sensitivity and specificity in the detection of spontaneous brain activity that is less susceptible to physiological noise (Zou et al., 2008). In the current study, this measure of fALFF in the posterior component of the DMN is shown to be susceptible to disruption in both normal aging and after an ischemic stroke. These findings may be attributable mainly to an age effect, as both the healthy older group and the subacute stroke patients were of an older age. However, the oscillations within the slow-5 oscillation band (0.01–0.027 Hz) may be additionally affected. Moreover, the reduction in spectral amplitude is not

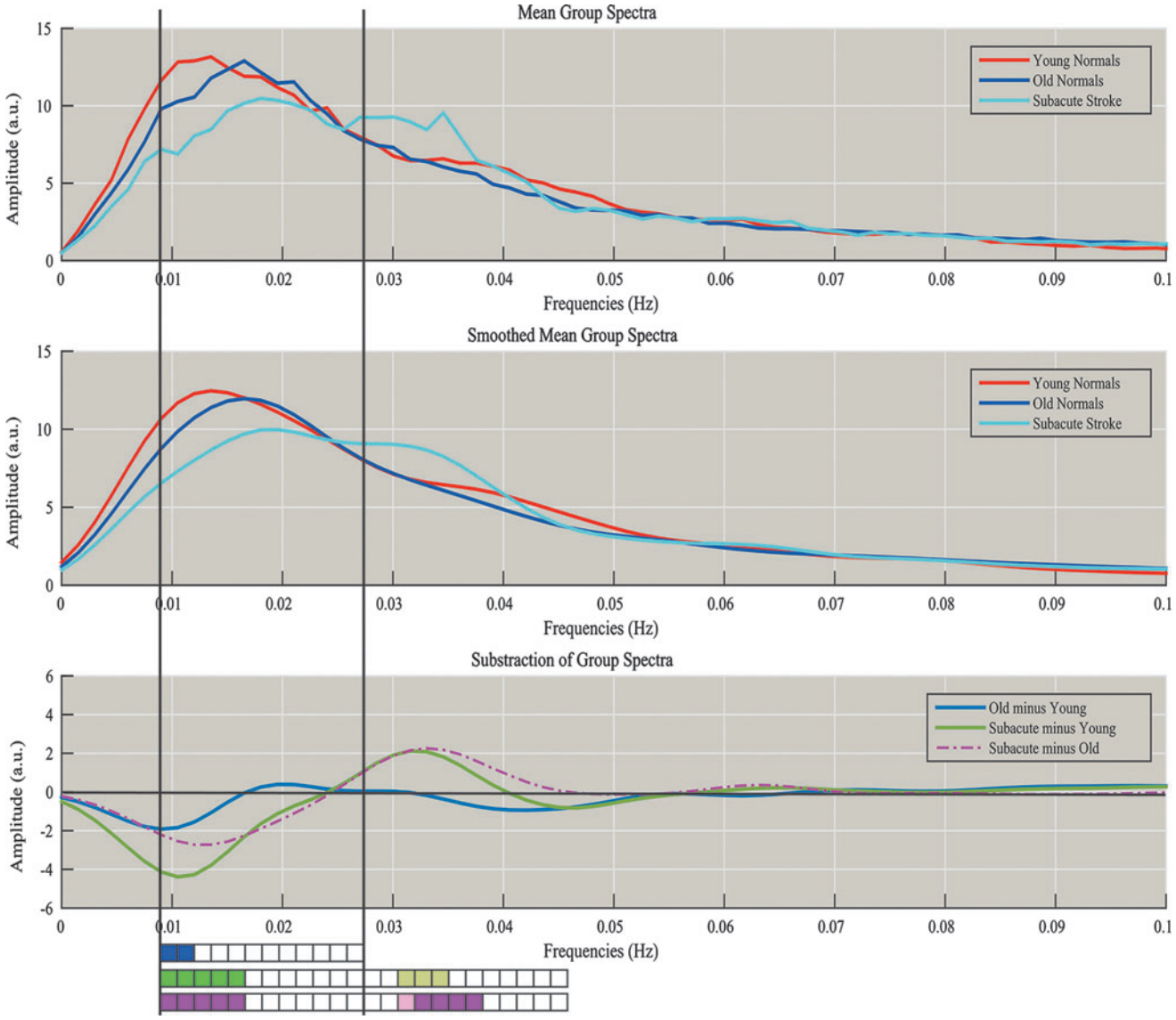

FIG. 7. Plot of the difference among mean group spectra. Top: Raw mean population spectra. Middle: Smoothed mean population spectra with Gaussian filter ($\sigma = 2$). Bottom: Blue denotes the subtraction of Old–Young, Green denotes the subtraction of Subacute–Young, and Purple denotes the subtraction of Subacute–Old. Rectangular boxes at the bottom represent series of statistical tests carried out between the population spectra for specific frequency bins, from 0.009 to 0.027 Hz (frequencies in the slow-5 range), and beyond from 0.027 to 0.045 Hz (some frequencies in the slow-4 range) in steps of $\sim$0.0015 Hz. Darkly colored boxes (blue, green, purple) denote statistical significance at $p < 0.05$, and lightly colored boxes (light green, pink) denote statistical significance trending toward $0.05 < p < 0.10$, with p-values uncorrected for multiple comparisons. There is a significant reduction in amplitude in slow-5 range in Old versus Young, with even greater reductions in amplitude noted in Subacute versus Young, and in Subacute versus Old. There is a trend toward significance and a significant increase in amplitude in the slow-4 range in Subacute versus Young, and in Subacute versus Old with no significant difference in amplitude noted in the Old versus Young comparison. The change from reduction in amplitude to an increase in amplitude when comparing Subacute versus Young and Subacute versus Old occurs at $\sim$0.024 Hz (near 0.027 Hz, the border of slow-5 vs. slow-4 range).

restricted to the pDMN, but it is apparent in other assessed networks as well (aDMN, vDMN, visual, and sensorimotor component) (Fig. 4). For the purpose of this investigation, only the primary component of the pDMN was considered.

In the posterior component of the DMN, our analysis of the fluctuation amplitudes of an individual subject's spectra using the fALFF metric indicated a lower power of the oscillations in the older adults (healthy and patients) within the resting-state frequencies, as compared with the young subjects (Fig. 5F). This finding of reduced power measures in the older population groups is consistent with previous reports of ALFF using voxel-wise approaches and supports the hypothesis of a general decline of network oscillation power with aging. These earlier studies described decreased ALFF within the DMN, more specifically over the region of the PCC with aging (Hu et al., 2014), in subjects with mild

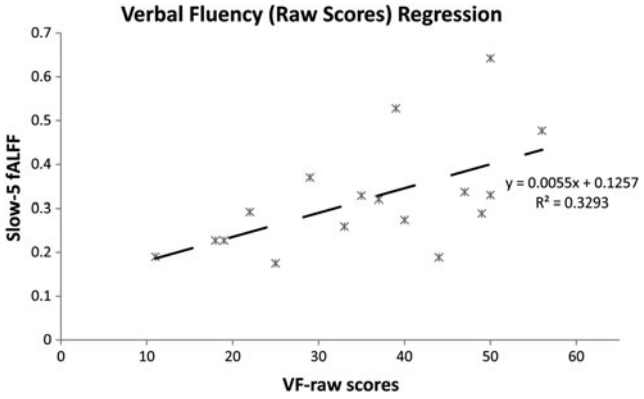

FIG. 8. Verbal fluency (raw scores) regression. Regression of out-of-scanner phonemic verbal fluency score with slow-5 fALFF values for subacute stroke patients, describing a linear trend between behavioral and neuronal measures ($R^2 = 0.329$, $F_{15} = 7.365$, $p = 0.016$).

cognitive impairment and Alzheimer's disease (Wang et al., 2011; Xi et al., 2012) and in stroke patients (Tsai et al., 2014). Though reduced fALFF was observed in the healthy older adults and with age as a potentially contributing factor, the impact of stroke injury on oscillations of the intrinsic network is not to be undermined. Aging may present an initial and progressive disruption of the network, whereas a stroke may impose a more dramatic reduction of those oscillation amplitudes, specifically in the slow-5 frequency range. Despite the fact that the disruption in frequency distribution observed in the subacute stroke population may have been partially confounded by a difference in age of the population, the effect in our subacute stroke population was more pronounced than in age-matched healthy control subjects, suggesting an exacerbation of the disruption in the event of a stroke. However, after the event of an injury, disruption of the network frequency distribution may be more specific than a general decline of oscillation power. A reduction specifically in the fractional power was particularly noted in the slow-5 oscillations (Figs. 3 and 6). This observation is in accordance with a previous report describing a high susceptibility of those slow-5 oscillations after the event of a stroke and the contribution of those oscillations to the cortical impairment (Zhu et al., 2015).

Our analysis also suggests that disruption after an acute injury, such as an ischemic stroke, may be linked to a change in the network distribution of cortical oscillation power among the sampled frequencies. Figure 3 illustrates a broader distribution of the cortical oscillation power within the pDMN component in the subacute stroke population as a group, extending beyond the slow-5 frequency range, which may help explain a possible mechanism underlying the impairment: through a disorganization of the network oscillations. The reductions in the slow-5 oscillations were often paired with an increase of the slow-4 oscillations (0.027–0.073 Hz), with no observed total fluctuation power difference as recorded by component fALFF over the resting-state frequencies (slow-5 + slow-4, 0.01–0.073 Hz), the adjacent frequency band, in comparison to the older healthy group. The ratio of slow-5 to resting-state oscillations was also altered in our subacute group (*post hoc* two-sample *t*-test, $p = 0.039$), demonstrating a weakening of the slow-5 oscillation in favor of the oscillations in the slow-4 range. These results present the possibility of a broadening of the spectral distribution through a reallocation of resources, with neurons potentially oscillating away from the slow-5 toward frequencies of those in the slow-4 range.

Discrete bin analysis within those oscillatory bands supported this observation (Fig. 7). We found lower oscillation power in the range of the slow-5 band and higher oscillation power in the slow-4 band once again, suggesting a progression to a broader distribution of oscillations as the system becomes impaired. The observations potentially reflect a certain vulnerability of the slow-5 oscillations, and a possible re-allocation of oscillation resources to the higher frequencies of the slow-4 in the impaired population after injury. Such a finding is accompanied by a potentially reduced overall resting-state ALFF in the older adults as compared with the younger adults whereas ALFF means between age-matched healthy and stroke populations did not differ, further contributing to the idea of oscillation resource re-allocation after cortical injury. This broadening of distribution may contribute to a reduction in the specificity of the information, with such diversity in oscillation frequency having a dramatic impact on the synchronization of the network and possibly impairing functions.

The subacute stroke patients, and to a lesser extent the older healthy adults, presented signs of diminished amplitude in distinct fluctuations within this slow-5 frequency range (Fig. 7), with the largest statistically significant difference in the bins of lower frequencies near the 0.012-Hz fluctuations (Fig. 7). Such a depression in the amplitude of those frequencies may have not only contributed, in part, to the appearance of the observed shifted peaks but also contributed to the reduced network coherence and synchronicity, allowing for long-distance communication between nodes of a network. In agreement with data presented in previous studies in aging-related pathologies (Han et al., 2011; Liu et al., 2014), these changes and differences observed in the slow-5 band of the resting state are indicative of a vulnerability of the slow-5 oscillations to disruption induced by the progression of normal aging and by the onset of an ischemic stroke.

Nonfractional estimate of power within those frequency ranges illustrated a similar reduction of slow-5 band in the subacute stroke population (Supplementary Fig. S2). Because fALFF is a fractional measure computed as the ratio of the power spectrum of the frequency of interest, to that of the entire frequency range, the change observed in slow-5 fALFF may have arisen from a reduction in slow-5 amplitude, an increase of slow-4 amplitudes, and/or an increase of the higher (0.073–0.192 Hz) frequencies. Figure 6 and Supplementary Fig. S2 demonstrate that an increase in slow-4 oscillation amplitude is plausible and may have contributed to the slow-5 fALFF observation. But again, we do suggest a re-allocation of oscillations to higher frequencies as a possible mechanism of the poststroke diaschisis effect. The most significant change in ALFF power remained within the slow-5 oscillation frequencies (Fig. 6), re-affirming the implication of the slow-5 oscillation in the network disruption. The reduction of slow-5 fALFF was likely not due to changes at the higher frequencies (0.073–0.192 Hz), as power in those frequencies is minimal. This was demonstrated in this study as well as in prior studies (Calhoun

et al., 2011; Zuo et al., 2010), Furthermore, low-TR fMRI (Kalcher et al., 2014) and MR-Encephalography (Lee et al., 2013) studies, techniques offering much improved temporal resolution, also confirmed the small contributions of high oscillations during the resting state.

Implications of slow-5 oscillation power

In healthy adult subjects, the slow-5 oscillations dominate the resting-state oscillations (Fig. 6), which is consistent with studies found in the literature (Garrity et al., 2007; Zuo et al., 2010). In contrast, our population of subacute stroke patients displayed a reduction in the amplitude and power that was specific to those slow-5 oscillations, which is consistent with results of a recent report by Zhu et al. (2015), where more activity changes were recorded in the ALFF of the slow-5 band. Our observation is coupled with an increase in slow-4 oscillations. Together, these observations contribute to the disruption of the balance between slow-5 and slow-4 oscillations of a healthy brain network, ultimately resulting in a reduction in network integrity.

The correspondence between slow-5 oscillation fALFF and behavior was seen in (1) a clinical measure assessing stroke severity—NIHSS and (2) a neuropsychological measure that assesses language and executive function—verbal fluency. Reduction of fALFF corresponded to worsening stroke severity and verbal fluency. This change in clinical and neuropsychological behavior may ultimately be a result of altered network integrity induced by a weakening of slow-5 oscillations.

However, the neuronal significance of those oscillations remains unclear. Arguments have been put forward to describe a potential association between those oscillations and EEG range oscillations, with the infra-slow oscillations (<0.1 Hz) providing amplitude envelops for concurrent higher-frequency oscillations (Goldman et al., 2002; Mantini et al., 2007). As the dominant oscillations of the infra-slow rs-fMRI resting-state fluctuations, slow-5 oscillations may provide such distinct amplitude envelopes underlying the opening and closing of temporal windows at the global, cortical scale, for coherently oscillating neuronal groups, and provide a modulation of alpha frequency signaling. Disruption of those oscillations may interrupt proper synchronization and transfer of information between distal, cortical areas of the same functional network. Hence, an assessment of the slow-5 frequency oscillations may provide a survey of network integrity and overall network health.

Spectral characteristic for the population of acute stroke

Behavior in the distribution of cortical oscillation power in the acute stroke patient group was not found to be significantly different from the younger or older healthy normals, with the spectral distribution for the acute patient group appearing more similar to that of the normal groups than the subacute stroke group (Fig. 4). This may be due to an absence of the diaschisis effect in the early time-point defined by our acute time window. The measure of fALFF recorded a slight increase in the acute population, representative of a possible power increase, which may have been due to an inhibitory deficit from impaired ''task-positive'' regions. Onset of an acute stroke may lead to release of inhibition from impaired networks to the DMN, with activation showing a temporary increase in amplitude and power measures before decreasing in the subacute stage (Figs. 4 and 5). However, changes observed in that population group remain minimal and are not significant in comparison to the other groups.

Limitations

Despite the novelty of the results, the current study has some limitations. Subjects' frequency distributions were particularly variable with the limited sample size, reducing the statistical significance of our results. Though the subacute group demonstrated the largest reduction, group-wise fALFF comparisons were only statistically significant in comparison to the younger group, which exhibited the lowest variance. We cannot exclude the possibility that the observed effect of a reduction of pDMN component fALFF may partially be a result of an age effect despite the presence of a control group of healthy, older individuals. Although a larger sample size for the stroke population and a more consistent window for the scanning of the subacute stroke population would most likely have improved the detection of the small effects in the spectral characteristics of the LFOs and benefited the characterization of the disruption, our investigation still presented evidence of disrupted slow-5 oscillations in the pDMN after a stroke.

Head motion, a concern in rs-fMRI, has not been directly addressed in this study, such as with the use of specific regression models. However, through the use of ICA, motion noise was identified and isolated into an independent component, reducing the influence of motion on signal from the independent components of interest (i.e., the pDMN). Furthermore, computation of motion Euclidean norm (enorm—square root of the sum squares) allowed an evaluation of the difference in motion among the groups (Supplementary Table S1). Head motion in the older healthy group was significantly higher than in the younger healthy group ($t_{70} = 3.145$, $p = 0.002$). Meanwhile, the differences in motion between the older groups (older healthy adults, acute stroke, and subacute stroke) were found not to be significant. Head motion is, therefore, unlikely to have substantially contributed to the current findings in oscillation amplitudes.

Nonuniformity of the stroke-induced lesions (demonstrated in Fig. 1) also limits the consistency of the functional and structural deficits in the study. To address this limitation, only selected networks and subnetworks were investigated here, with focus on the posterior component of the DMN, our most robust component. Comprising anatomically deeper core regions and not a commonly observed stroke location, the pDMN is an ideal candidate for the investigation of diaschisis effect from stroke on network alteration. Given that the DMN is known to interact in a similar fashion with various brain networks, investigation of this specific subnetwork would likely reduce the influence of lesion nonhomogeneity (i.e., lesions affecting various networks) found in our stroke patients on disruption of network oscillations.

The large variation in the time of assessment for the subacute stroke group may also have contributed to the large deviation in power spectra. However, our results suggest a larger role of the sample size than variability of scanning time in the variability of the component slow-5 fALFF, since acute and subacute groups demonstrated similar variability in the measure of slow-5 fALFF (healthy younger

and healthy older adults had nearly half the variability; Group Std. Err.: Young: 0.016, Old: 0.018, Acute: 0.033, Subacute: 0.029). A larger study of power spectra in stroke patients would be important in further evaluating these results. A plausible influence of assessment time on slow-5 fALFF is also a possibility. Regression of days of onset to slow-5 fALFF provided a weak association between the two measures ($R^2 = 0.149$, $F_{16} = 2.81$, $p = 0.11$), suggesting that future investigations would benefit from a better control for time of assessment to determine the level of slow-5 disruption. This does not, however, dissuade one from the evidence provided for reduced slow-5 activity after the event of a stroke.

The current findings could have also been confounded with cerebrovascular reactivity (CVR) status differences among the populations/CVR in the stroke group may be altered in comparison to healthy adults, since stroke is a vascular injury. However, little is known regarding the correction for CVR, in particular within the resting-state signal, and is, therefore, not directly addressed in this investigation. Physiological noises such as cardiac and respiratory signal have not been systematically measured, though such contributions have been suggested to influence fluctuations at higher frequencies outside of the slow-5 oscillation range: 0.04 Hz for hypercapnic conditions induced by breath hold (Biswal et al., 2007), and 0.03 Hz for respiratory variations (Birn et al., 2006).

Those physiological signals would also have influenced the resting-state oscillations equally among the populations, not contributing to group differences in the oscillation amplitudes. Furthermore, ICA has been found to be relatively robust to respiration-related fluctuations, separating respiration-volume variations into separate components (Birn et al., 2008). Despite the nondominance of slow-4 oscillations in the healthy adult resting state, this investigation could have benefited from a more thorough exploration of the slow-4 oscillations, but because of the lack of physiological recording, known sources of noise within that frequency range, further work needs to be done to explain changes observed within this particular frequency range.

Despite these limitations, with this investigation, we have provided evidence of a reduction in slow-5 oscillation amplitude found in stroke patients in their subacute stage, which may be associated with stroke severity (NIH-SS) and reduced performance in a behavioral task (verbal fluency), potentially from an altered network connectivity induced by a stroke diaschisis effect. This modification of oscillation amplitude could have dramatic influences on the balance of intrinsic oscillation, contributing to the functionality and integrity of the DMN network with oscillations in the slow-5 frequency range decreasing in their dominance of the resting-state fluctuations. The repeated identification of slow-5 frequencies in the current study and other previous studies (Calhoun et al., 2011; Han et al., 2011; Yu et al., 2014; Zhu et al., 2015) stresses the critical role of the slow-5 oscillation in network disruption, and it also accentuates the importance of managing slow-5 oscillations in the health of the DMN. More studies are needed to validate the current findings and to determine their possible clinical significance.

Conclusion

Despite the large variance in the resting-state oscillation characteristics and the presence of other differences such as medications, comorbidities, vascular risk factors, and/or chronic perfusion problems in our stroke population compared with our healthy adults, this study provided evidence that the normal functioning of the DMN is disrupted in the ischemic stroke group with an effect on the distribution of intrinsic oscillations. In the pDMN component, age-related changes and stroke-related changes appear to have a distinct influence on the amplitude of the oscillations in the slow-5 frequency range, which might have contributed to the appearance of a shifted peak (higher mean frequency of the peak in older populations).

It remains unclear whether the disruption of the DMN is primarily driven by a reduction in amplitude of the oscillations at specific frequencies and/or by a modification of the network oscillation frequency distribution, reducing the synchronization among the nodes of the network. In the subacute stroke group, this effect is accompanied by an increase in oscillation power in the slow-4 frequency range, contributing to a change in the balance of slow-5 to slow-4. This latter effect may offer potential insight into mechanisms of brain plasticity after stroke injury. Ultimately, the results of our study stress the importance of managing slow-5 oscillations in the health of the DMN, and they suggest the potential of slow-5 band oscillations as an indicator of alterations in the DMN with aging, stroke, and in other disease processes.

Acknowledgments

The project described was partly supported by the Clinical and Translational Science Award (CTSA) program, through the NIH National Center for Advancing Translational Sciences (NCATS) grant UL1TR000427, the NTP training grant T32-GM007507, the CNTP training grant T32EB011434, the Medical Scientist Training Program NIH grant T32GM008692, and NIH grants RC1MH090912 and K23NS086852, the American Heart Association, Foundation of ASNR, and Shapiro Foundation Grants. The content is solely the responsibility of the authors and does not necessarily represent the official views of the NIH.

Author Disclosure Statement

No competing financial interests exist.

References

Allen EA, Erhardt EB, Damaraju E, Gruner W, Segall JM, Silva RF, et al. 2011. A baseline for the multivariate comparison of resting-state networks. Front Syst Neurosci 5:2.

Andrews-Hanna JR, Reidler JS, Sepulcre J, Poulin R, Buckner RL. 2010. Functional-anatomic fractionation of the brain's default network. Neuron 65:550–562.

Andrews-Hanna JR, Snyder AZ, Vincent JL, Lustig C, Head D, Raichle ME, et al. 2007. Disruption of large-scale brain systems in advanced aging. Neuron 56:924–935.

Bai F, Zhang Z, Yu H, Shi Y, Yuan Y, Zhu W, et al. 2008. Default-mode network activity distinguishes amnestic type mild cognitive impairment from healthy aging: a combined structural and resting-state functional MRI study. Neurosci Lett 438:111–115.

Beckmann CF, DeLuca M, Devlin JT, Smith SM. 2005. Investigations into resting-state connectivity using independent component analysis. Philos Trans R Soc Lond B Biol Sci 360:1001–1013.

Bell AJ, Sejnowski TJ. 1995. An information-maximization approach to blind separation and blind deconvolution. Neural Comput 7:1129–1159.

Birn RM, Diamond JB, Smith MA, Bandettini PA. 2006. Separating respiratory-variation-related fluctuations from neuronal-activity-related fluctuations in fMRI. Neuroimage 31: 1536–1548.

Birn RM, Molloy EK, Patriat R, Parker T, Meier TB, Kirk GR, et al. 2013. The effect of scan length on the reliability of resting-state fMRI connectivity estimates. Neuroimage 83:550–558.

Birn RM, Murphy K, Bandettini PA. 2008. The effect of respiration variations on independent component analysis results of resting state functional connectivity. Hum Brain Mapp 29:740–750.

Biswal B, Zerrin Yetkin F, Haughton VM, Hyde JS. 1995. Functional connectivity in the motor cortex of resting human brain using echo-planar mri. Magn Reson Med 34:537–541.

Biswal BB, Kannurpatti SS, Rypma B. 2007. Hemodynamic scaling of fMRI-BOLD signal: validation of low-frequency spectral amplitude as a scalability factor. Magn Reson Imaging 25:1358–1369.

Broyd SJ, Demanuele C, Debener S, Helps SK, James CJ, Sonuga-Barke EJ. 2009. Default-mode brain dysfunction in mental disorders: a systematic review. Neurosci Biobehav Rev 33:279–296.

Buckner RL, Andrews-Hanna JR, Schacter DL. 2008. The brain's default network. Ann N Y Acad Sci 1124:1–38.

Buzsáki G, Draguhn A. 2004. Neuronal oscillations in cortical networks. Science 304:1926–1929.

Calhoun VD, Sui J, Kiehl K, Turner J, Allen E, Pearlson G. 2011. Exploring the psychosis functional connectome: aberrant intrinsic networks in schizophrenia and bipolar disorder. Front Psychiatry 2:75.

Chao-Gan Y, Yu-Feng Z. 2010. DPARSF: A MATLAB toolbox for ''pipeline'' data analysis of resting-state fMRI. Front Syst Neurosci 4:13.

Damoiseaux J, Beckmann C, Arigita ES, Barkhof F, Scheltens P, Stam C, et al. 2008. Reduced resting-state brain activity in the ''default network'' in normal aging. Cereb Cortex 18:1856–1864.

Damoiseaux J, Rombouts S, Barkhof F, Scheltens P, Stam C, Smith SM, et al. 2006. Consistent resting-state networks across healthy subjects. Proc Natl Acad Sci U S A 103:13848–13853.

Ferreira LK, Busatto GF. 2013. Resting-state functional connectivity in normal brain aging. Neurosci Biobehav Rev 37:384–400.

Fox MD, Raichle ME. 2007. Spontaneous fluctuations in brain activity observed with functional magnetic resonance imaging. Nat Rev Neurosci 8:700–711.

Fransson P. 2005. Spontaneous low-frequency BOLD signal fluctuations: An fMRI investigation of the resting-state default mode of brain function hypothesis. Hum Brain Mapp 26:15–29.

Friston K, Frith C, Liddle P, Frackowiak R. 1993. Functional connectivity: the principal-component analysis of large (PET) data sets. J Cereb Blood Flow Metab 13:5–5.

Garrity AG, Pearlson GD, McKiernan K, Lloyd D, Kiehl KA, Calhoun VD. 2007. Aberrant ''default mode'' functional connectivity in schizophrenia. Am J Psychiatry 164:450–457.

Goldman RI, Stern JM, Engel Jr. J, Cohen MS. 2002. Simultaneous EEG and fMRI of the alpha rhythm. Neuroreport 13: 2487.

Grady CL, Springer MV, Hongwanishkul D, McIntosh AR, Winocur G. 2006. Age-related changes in brain activity across the adult lifespan. J Cogn Neurosci 18:227–241.

Greicius M. 2008. Resting-state functional connectivity in neuropsychiatric disorders. Curr Opin Neurol 21:424–430.

Greicius MD, Srivastava G, Reiss AL, Menon V. 2004. Default-mode network activity distinguishes Alzheimer's disease from healthy aging: evidence from functional MRI. Proc Natl Acad Sci U S A 101:4637–4642.

Gusnard DA, Akbudak E, Shulman GL, Raichle ME. 2001a. Medial prefrontal cortex and self-referential mental activity: relation to a default mode of brain function. Proc Natl Acad Sci U S A 98:4259–4264.

Gusnard DA, Raichle ME, Raichle ME. 2001b. Searching for a baseline: functional imaging and the resting human brain. Nat Rev Neurosci 2:685–694.

Han Y, Wang J, Zhao Z, Min B, Lu J, Li K, et al. 2011. Frequency-dependent changes in the amplitude of low-frequency fluctuations in amnestic mild cognitive impairment: a resting-state fMRI study. Neuroimage 55:287–295.

He Y, Wang L, Zang Y, Tian L, Zhang X, Li K, et al. 2007. Regional coherence changes in the early stages of Alzheimer's disease: a combined structural and resting-state functional MRI study. Neuroimage 35:488–500.

Himberg J, Hyvärinen A, Esposito F. 2004. Validating the independent components of neuroimaging time series via clustering and visualization. Neuroimage 22:1214–1222.

Hu S, Chao HH, Zhang S, Ide JS, Li CS. 2014. Changes in cerebral morphometry and amplitude of low-frequency fluctuations of BOLD signals during healthy aging: correlation with inhibitory control. Brain Struct Funct 219:983–994.

Johnson SC, Schmitz TW, Kawahara-Baccus TN, Rowley HA, Alexander AL, Lee J, et al. 2005. The cerebral response during subjective choice with and without self-reference. J Cogn Neurosci 17:1897–1906.

Kalcher K, Boubela RN, Huf W, Bartova L, Kronnerwetter C, Derntl B, et al. 2014. The spectral diversity of resting-state fluctuations in the human brain. PLoS One 9:e93375.

Koch W, Teipel S, Mueller S, Buerger K, Bokde AL, Hampel H, et al. 2010. Effects of aging on default mode network activity in resting state fMRI: does the method of analysis matter? Neuroimage 51:280–287.

Lee HL, Zahneisen B, Hugger T, LeVan P, Hennig J. 2013. Tracking dynamic resting-state networks at higher frequencies using MR-encephalography. Neuroimage 65:216–222.

Liu X, Wang S, Zhang X, Wang Z, Tian X, He Y. 2014. Abnormal amplitude of low-frequency fluctuations of intrinsic brain activity in Alzheimer's disease. J Alzheimers Dis 40: 387–397.

Mantini D, Perrucci MG, Del Gratta C, Romani GL, Corbetta M. 2007. Electrophysiological signatures of resting state networks in the human brain. Proc Natl Acad Sci U S A 104:13170–13175.

Meinzer M, Seeds L, Flaisch T, Harnish S, Cohen ML, McGregor K, et al. 2012. Impact of changed positive and negative task-related brain activity on word-retrieval in aging. Neurobiol Aging 33:656–669.

Park JY, Kim YH, Chang WH, Park CH, Shin YI, Kim ST, et al. 2014. Significance of longitudinal changes in the default-mode network for cognitive recovery after stroke. Eur J Neurosci 40:2715–2722.

Patriat R, Molloy EK, Meier TB, Kirk GR, Nair VA, Meyerand ME, et al. 2013. The effect of resting condition on resting-state fMRI reliability and consistency: a comparison between resting with eyes open, closed, and fixated. Neuroimage 78:463–473.

Penttonen M, Buzsáki G. 2003. Natural logarithmic relationship between brain oscillators. Thalamus Relat Syst 2:145–152.

Persson J, Lustig C, Nelson JK, Reuter-Lorenz PA. 2007. Age differences in deactivation: a link to cognitive control? J Cogn Neurosci 19:1021–1032.

Qin P, Northoff G. 2011. How is our self related to midline regions and the default-mode network? Neuroimage 57:1221–1233.

Raichle ME. 2010. Two views of brain function. Trends Cogn Sci 14:180–190.

Raichle ME, MacLeod AM, Snyder AZ, Powers WJ, Gusnard DA, Shulman GL. 2001. A default mode of brain function. Proc Natl Acad Sci U S A 98:676–682.

Sambataro F, Murty VP, Callicott JH, Tan H-Y, Das S, Weinberger DR, et al. 2010. Age-related alterations in default mode network: impact on working memory performance. Neurobiol Aging 31:839–852.

Schmitz TW, Kawahara-Baccus TN, Johnson SC. 2004. Metacognitive evaluation, self-relevance, and the right prefrontal cortex. Neuroimage 22:941–947.

Tsai Y-H, Yuan R, Huang Y-C, Yeh M-Y, Lin C-P, Biswal BB. 2014. Disruption of brain connectivity in acute stroke patients with early impairment in consciousness. Front Psychol 4:956.

Tuladhar AM, Snaphaan L, Shumskaya E, Rijpkema M, Fernandez G, Norris DG, et al. 2013. Default mode network connectivity in stroke patients. PLoS One 8:e66556.

Van Dijk KR, Hedden T, Venkataraman A, Evans KC, Lazar SW, Buckner RL. 2010. Intrinsic functional connectivity as a tool for human connectomics: theory, properties, and optimization. J Neurophysiol 103:297–321.

Wagner AD, Shannon BJ, Kahn I, Buckner RL. 2005. Parietal lobe contributions to episodic memory retrieval. Trends Cogn Sci 9:445–453.

Wang C, Qin W, Zhang J, Tian T, Li Y, Meng L, et al. 2014. Altered functional organization within and between resting-state networks in chronic subcortical infarction. J Cereb Blood Flow Metab 34:597–605.

Wang Z, Yan C, Zhao C, Qi Z, Zhou W, Lu J, et al. 2011. Spatial patterns of intrinsic brain activity in mild cognitive impairment and Alzheimer's disease: a resting-state functional MRI study. Hum Brain Mapp 32:1720–1740.

Xi Q, Zhao X, Wang P, Guo Q, Yan C-G, He Y. 2012. Functional MRI study of mild Alzheimer's disease using amplitude of low frequency fluctuation analysis. Chin Med J (Engl) 125:858–862.

Yang H, Long X-Y, Yang Y, Yan H, Zhu C-Z, Zhou X-P, et al. 2007. Amplitude of low frequency fluctuation within visual areas revealed by resting-state functional MRI. Neuroimage 36:144–152.

Yu R, Chien YL, Wang HL, Liu CM, Liu CC, Hwang TJ, et al. 2014. Frequency-specific alternations in the amplitude of low-frequency fluctuations in schizophrenia. Hum Brain Mapp 35:627–637.

Yu-Feng Z, Yong H, Chao-Zhe Z, Qing-Jiu C, Man-Qiu S, Meng L, et al. 2007. Altered baseline brain activity in children with ADHD revealed by resting-state functional MRI. Brain Dev 29:83–91.

Zhang Z, Liu Y, Jiang T, Zhou B, An N, Dai H, et al. 2012. Altered spontaneous activity in Alzheimer's disease and mild cognitive impairment revealed by Regional Homogeneity. Neuroimage 59:1429–1440.

Zhu J, Jin Y, Wang K, Zhou Y, Feng Y, Yu M, et al. 2015. Frequency-Dependent Changes in the Regional Amplitude and Synchronization of Resting-State Functional MRI in Stroke. PLoS One 10:e0123850.

Zou Q-H, Zhu C-Z, Yang Y, Zuo X-N, Long X-Y, Cao Q-J, et al. 2008. An improved approach to detection of amplitude of low-frequency fluctuation (ALFF) for resting-state fMRI: fractional ALFF. J Neurosci Methods 172:137–141.

Zuo X-N, Di Martino A, Kelly C, Shehzad ZE, Gee DG, Klein DF, et al. 2010. The oscillating brain: complex and reliable. Neuroimage 49:1432–1445.

Address correspondence to:
Christian La
Department of Radiology
Wisconsin Institute of Medical Research (WIMR), 1310-L
1111 Highland Avenue
Madison, WI 53705

E-mail: cla@wisc.edu